Científica, vol. 29, núm. 1, pp. 01-15, enero-junio 2025, ISSN 2594-2921, Instituto Politécnico Nacional, MÉXICO
e290110 | DOI: 10.46842/ipn.cien.v29n1a10

ARTICLE

Preparation pressure effects on proposed thermoluminiscent gamma radiation detectors fabricated from single wall carbon nanotubes (SWCNT)

Análisis de los efectos de la presión de fabricación de pastillas de nanotubos de carbono de pared simple como posible detector termoluminiscente de radiación gamma

Alejandro **Ortiz Morales**[1], Jaime **Ortiz López**[2], Benjamín **Leal Acevedo**[3], Ramón **Gómez Aguilar**[4]

Instituto Politécnico Nacional,
Unidad Profesional Interdisciplinaria en Ingeniería y Tecnologías Avanzadas, Ciudad de México, MÉXICO
[1]ORCID: 0000-0002-6897-0789 | alortizm@ipn.mx *Corresponding author
Escuela Superior de Física y Matemáticas, Ciudad de México, MÉXICO
[2]ORCID: 0000-0002-9958-619X | jortizl@ipn.mx
[4]ORCID: 0000-0002-5945-5929 | rgomeza@ipn.mx

Universidad Nacional Autónoma de México,
Instituto de Ciencias Nucleares, Unidad de Irradiación y Seguridad Radiológica, Ciudad de México, MÉXICO
[3]ORCID: 0009-0005-4464-892X | benjamin.leal@nucleares.unam.mx

Recibido 26/03/2025, aceptado 25/06/2025.

Abstract

Single wall carbon nanotube (SWCNT) pellets have been manufactured at pressures of 1, 2.5 and 5 Tons, and later exposed to gamma photons from a Co^{60} source to study their thermoluminiscent (TL) properties. SWCNT were synthesized by the electric arc discharge technique and pellets were characterized with Raman spectroscopy, X-ray diffraction (XRD) and scanning electron microscopy (SEM). The effective atomic number (Z_{eff}) of these pellets has a value of 15.08 like the one of human bones. The pellets were exposed to a gamma irradiation dose ranging from 1.0 to 100 [kGy]. The kinetic parameters, activation energy *E*, frequency factor *s*, kinetic order *b*, are obtained from a structure of glow curve using deconvolution and heuristic equations (Chen, Lushchik, Balarin, etc.) give us information of the mechanisms responsible of the TL signal in SWCNT-pellets, which is due to recombination of electron–hole pairs. The main glow peak is observed at 452, 465 and 477 K, in samples A, B and C, respectively. As preparation pressure pellets increases, activation energy decreases for all traps in the samples, indicating the creation of defects in the SWCNT structure. Three stages are displayed in the TL dose-response for all samples, and linearity was maintained up to 2.5 kGy. Thermoluminescence, X-RD, scanning electron microscopy and Raman scattering, analyses show that pellet A is a promising high radiation detector.

Index words: single wall carbon nanotube pellets, thermoluminescence, scanning electron microscopy, pellet preparation pressure, X-ray diffraction, Raman spectroscopy, radiation gamma detector.

Resumen

Pastillas de nanotubos de carbono de pared simple (SWCNT) se fabricaron a las presiones de 1, 2.5 y 5 toneladas, posteriormente se irradiaron con fotones gamma de una fuente de Co^{60} con el objetivo de estudiar sus propiedades termoluminiscentes (TL). Los nanotubos de pared simple se sintetizaron mediante la técnica de descarga de arco eléctrico y se caracterizaron con espectroscopia Raman, difracción de rayos X (D R-X) y microscopía electrónica de barrido (SEM). El número atómico efectivo (Z_{eff}) de los nanotubos tiene un valor de 15.08 similar al de los huesos humanos. Las pastillas se expusieron a una dosis de irradiación gamma que variaba de 1.0 a 100[kGy]. Los parámetros cinéticos, energía de activación E, factor de frecuencia s, orden cinético b, se obtienen a partir de la estructura de la curva de brillo usando deconvolución y ecuaciones heurísticas (Chen, Lushchik, Balarin, etc.) que brindan información de los mecanismos responsables de la señal TL en las pastillas de SWCNT la recombinación de pares electrón-hueco. El pico de brillo principal está localizado a 452, 465 y 477 K, en las muestras A, B y C, respectivamente. Conforme aumenta la presión de fabricación, la energía de activación disminuye para todas las trampas en las muestras, lo que indica la creación de defectos en la estructura de los nanotubos de carbón de pared simple. Se muestran tres etapas en la respuesta TL-dosis para todas las muestras, y la linealidad se mantuvo hasta 2.5 kGy. Los análisis con termoluminiscencia, difracción de rayos X, microscopía electrónica de barrido y dispersión Raman muestran que la pastilla A es un detector de radiación gamma, prometedor en el intervalo de dosis analizado.

Palabras clave: nanotubos de pared simple, termoluminiscencia, microscopía electrónica de barrido, presión de preparación de pastillas, difracción de rayos X, espectroscopia Raman, detector de radiación gamma.

I. Introduction

A vast variety of materials such as PPV-polymer derivative films and doped metallic oxides have been analyzed with luminescence heat stimulation, aiming to their use as thermoluminiscent (TL) detectors [1][2][3]. Recently, SWCNT in powder form was shown to exhibit thermoluminiscent properties [4]. In recent years [5] manufacture TL material, $CaSO_4$: X, where X: Rare earths, such as: Dy, Tm, Eu, in pellets form, have been proposed for TL dosimeters for their properties such as: reproducibility, linear dose response, low fading of the TL signal, etc. Mathur *et al* [6], analyzed $CaSO_4$: Dy-pellets, using TL-phenomenon concluding; molar concentration of 1 and 2 %, coadyuvate notably in the TL curve (peaked at 335 and 475 ^{0}C) increasing the range of dose (100- 500 kGy). Tarawneh *et al* [7], realized studies with hybrid carbon nanotubes and montmorillonite nanocomposites, improve physical properties and optimize the effect of gamma dose until 150 kGy. Sobczak *et al* [8], used multiwall carbon nanotubes (MWCNT) to manufacture MWCNT/paraffin nanocomposites finding that high concentration of CNTs and iron encapsulates magnify the response before gamma radiation fields. The excellent response of SWCNTs to high doses of gamma radiation represents a valuable opportunity for technological applications. The SWCNT-pellets could be interesting for measuring doses at gamma irradiation plant in which services are done to ensure the debacterization, sanitization and safety of various products such as dehydrated foods, medical-disposable devices, pharmaceuticals, cosmetics, herbalists, etc. Gamma irradiation is one of the most effective procedures for food preservation, comparable to pasteurization, canning or freezing. The nature of this radiation energy breaks the DNA chains of harmful microorganisms and manages to pass through the packaging of the product without altering its internal or external structure [9]. Carbon nanotube-based devices are excellent candidates for lightweight personal dosimeters. They are highly sensitive sensors, display particularly low power consumption [10] and have already shown promising applications in X-ray dosimetry [11]. Chemical functionalization of SWCNT can be used to increase a sensor's physical and chemoselective sensitivity. There has been substantial effort in the functionalization of SWCNTs to alter both their electronic properties and dispersibility as well as to obtain desirable properties for radiation sensing [12][13]. In the interest of developing real time, memory free sensors, radiation tolerance of the sensing material is a key factor. It has been demonstrated previously that unfunctionalized SWCNT's are radiation tolerant, [14] [15] because of the inherent strength of the aromatic C-C bonds. Depending on physical state (powder, pellets or buckypaper) it can establish a linearity range for commercial use like a TL-detector of high dose rate fields.

Gspann *et. al* 2018 [16], reports during tensile test of SWCNT, triboluminescence flashes occurring at the fracture sites that depend on the sample morphology caused by charge separation due to SWCNT bond fracture and gas discharge of the surrounding gases. Before SWCNT pellets are exposed to a source of ionizing radiation, triboluminescence has already occurred. For SWCNT material, the ratio between the conducting and semiconducting CNT is 1:2 and that semiconducting species show a band gap with an energy depending on diameter/chirality ratio. In SWCNTs were found to emit light from interband recombination of electron–hole pairs [17].

The objective of this paper is to analyze the effect of different manufacturing pressures on SWCNT pellets and to correlate these conditions with TL kinetic parameters (activation energy ***E***, frequency factor ***s*** and kinetic order ***b)*** to evaluate their application like a gamma ray detector.

II. Method

Single wall carbon nanotubes (SWCNT) were synthesized at the (IPN-ESFM) with a modified electric arc discharge technique [18] under hydrogen atmosphere (200 Torr) using the following catalytic mixture in powder form: of C/Ni/Co/Fe/FeS in 95.25/2.6/0.7/0.7/0.75 molar concentrations, respectively. With this technique and catalytic mixture composition, SWNT are synthesized with diameters in the 1 to 2 nm range. Briefly, a DC current of 150 A is supplied by a 22.8 kVA commercial arc welding equipment externally connected to a bell jar evaporator which is used a s a growth chamber. Inside the bell-jar an electric arc discharge is maintained between the tip of a sharpened graphite cathode and an anode formed by the catalytic mixture. These powders are compressed inside cavities carved on a supporting graphite block. The cathode is placed with an inclination of about 60° above the filled cavities so that the plasma jet of the discharge is deviated towards the empty volume of the growth chamber. After the discharge is triggered, SWCNT bundles are obtained in the form of a black web-like material that grows and hangs from objects inside the chamber and as a fluffy black film deposited on the chamber walls. Pellets designated as A, B and C were made with a manual hydraulic press with SWCNT initially in powder form applying 1, 2.5 and 5-ton pressure, respectively, at room temperature and 1atm. The black colored disk-shaped pellets are 5 mm in diameter

0.5 mm in thickness and 30 mg in weight. Annealing treatments were performed by heating the samples at 770 K for 1 h and then dropping them onto a copper block at room temperature (RT). The pellets were exposed to gamma photons from ^{60}Co irradiator (Gammabeam 651-PT) with a 152 Gy/min dose rate at the Nuclear Science Institute-UNAM facilities. Dosimetric characterization was also performed in UNAM with a Harshaw TLD model 3500 TL reader system at a constant heating rate of 2 K/s under nitrogen atmosphere to eliminate any spurious signals.

SWCNT-pellets were characterized by scanning electron microscopy (SEM). Using a JSM-7900 F instrument at the Centro Nanociencias and Micro-Nanotecnologias of IPN (IPN-CNMN) operated at 1.5 kV with secondary electrons. XRD patterns were obtained with a PANalytical diffractometer, model X Pert PRO MRD using Cu-K_α radiation (λ= 1.5404 Å) operated at 45 kV and 40mA at IPN-CNMN. Raman scattering spectroscopy characterization was performed also at IPN with a Horiba Jobin Yvon LabRaman HR-800 instrument with 633 nm (1.958 eV) excitation.

III. Results

A. Scanning electron microscopy(SEM) of SWCNT pellets

Fig.1 Shows a SEM image of bundles of SWCNT's synthesized by electric arc discharge before the fabrication of pellets. As shown elsewhere [18], the synthesized material consists of SWCNT's with diameters in the range of 1 to 2 nm. Figure 1 shows, however, that the SWCNTs actually cluster into bundles made up of different numbers of individual SWCNTs, giving the bundles a wide distribution of diameters. The table indicates measured lengths of various bundles identified by index numbering 1 to 11. Also shown is a magnified view of one of these bundles indicating a measured diameter of 0.066 μm surrounded by other SWCNT bundles having different diameters. The measured bundle is formed by about 30 to 60 individual SWCNTs.

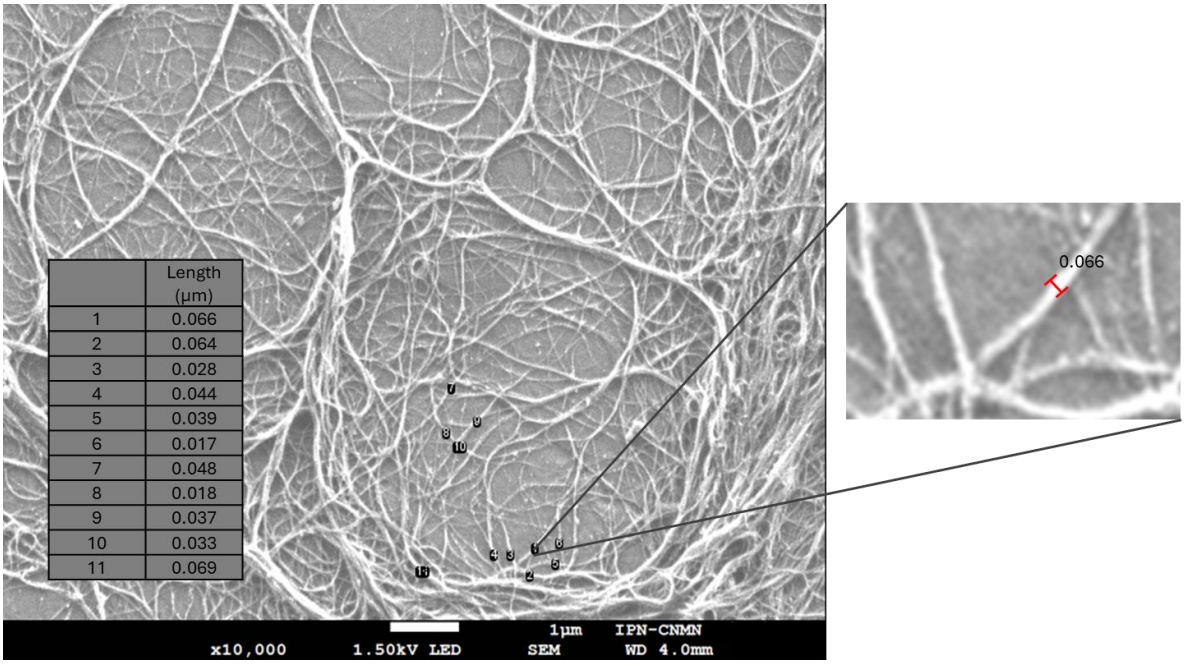

Fig. 1. SEM image of bundles of synthesized SWCNT as produced with electric arc discharge technique [18]. Individual SWCNT of 1 to 2 nm diameter cluster into bundles formed by different numbers of SWCNTs resulting in bundles with a wide distribution of diameters. Magnified view of a selected bundle of 0.066 μm diameter.

B. X-ray and Raman characterization of SWNT pellets

Diffraction patterns of pellet A before and after gamma-ray exposure are shown in Fig. 2. Both patterns are normalized to the most prominent peak (P1) intensity around 2θ = 26.4° which is identified as the (002) reflection of graphitic materials with hexagonal crystalline structure. Other peaks expected from sp^2 carbons are (101) and (004) reflections which are coincident with peaks P2 and P4, respectively. The weakest peak P3 main contributions are due to the presence of catalytic metal residues, mainly Ni and Ni, Fe and Co carbides. Other catalytic metal residues (Fe, Ni, Co),

their carbides and alloys, may also contribute to all P1-P4 peaks as shown in the lower part of Fig. 2 where the position of diffraction peaks (as reported in the indicated JCPDS-PDF cards) of phases expected to be present in the sample are indicated. Peak positions for carbon nanotube bundles, as reported in [19] and JCPDS 00-058-1638 (CNT in Fig. 2), are also consistent with our measured patterns. Due to the disordered state of compressed SWCNT bundles and heterogeneous nature of the sample, diffraction peaks are inhomogeneously broadened and difficult to analyze for strict phase identification and quantification. The slight increase in the background signal for the irradiated sample, is presumably due to defect formation and partial amorphization of the sample by gamma-rays, otherwise the diffraction peaks remain nearly unaffected before and after irradiation. Because the diffractograms of all samples are almost identical, we only show the most significant ones.

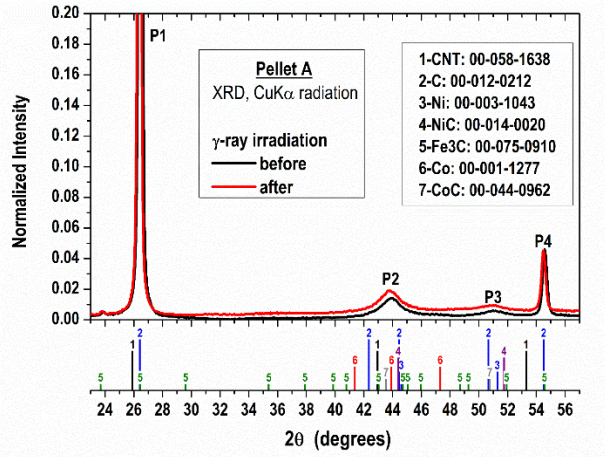

Fig. 2. X-ray diffraction patterns (normalized with respect to intensity of peak P1) of pellet A before and after gamma-ray irradiation. Vertical scale is chosen so that smaller peaks are adequately recognized. The position of diffraction peaks of phases expected to be present in the sample are shown in the lower part, according to the indicated JCPDS-PDF database cards.

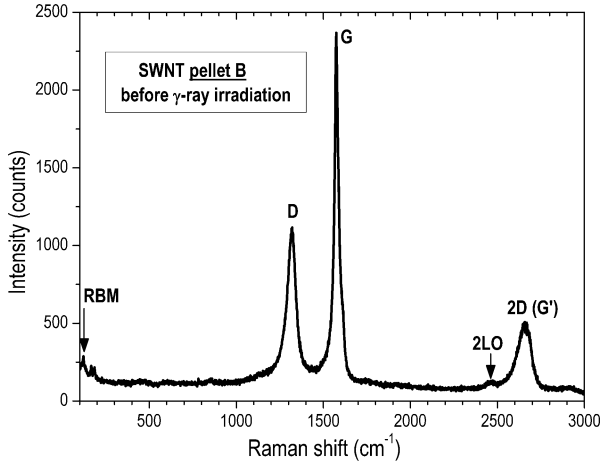

Fig. 3. Raman spectrum of the non-irradiated compressed pellet B prepared with 2.5-ton pressure.

Científica, vol. 29, núm. 1, pp. 01-15, enero-junio 2025, ISSN 2594-2921, Instituto Politécnico Nacional, México
e290110 | doi: 10.46842/ipn.cien.v29n1a10

As shown in Fig. 3 a typical Raman spectrum of pellet B before irradiation. Spectra taken at different points on the surface of the pellet do not exhibit great differences in spectral features. A series of weak peaks corresponding to radial breathing modes (RBM) of SWCNTs are observed at low frequency. The most prominent around 122 cm^{-1} corresponds to SWCNTs with ~2.08 nm diameter (calculated with $\omega_{RBM}=234/d + 10$ where ω_{RBM} is in cm^{-1} and d in nm, see Shimada, et. al., 2005) [20] which are expected to be semiconducting SWCNTs. The peak around 1320 cm^{-1} is the so-called disorder-induced D band associated with structural defects and deformations of the SWNT bundles. The band located around 1580 cm^{-1}, known as the G band, is associated to tangential vibrational modes of the SWCNT. At high frequency, second order Raman bands around 2450 and 2650 cm^{-1} are assigned to overtone modes: the first to a LO phonon mode (2LO), and the second to the overtone of the D band (2D also known as G'), respectively. It should be noted that the Raman spectra of raw synthesized SWNT in powder form [18] shows no evidence of the 2LO band, and the D band is weaker with respect to G band intensity, with a ratio I_D/I_G in the range 0.20 to 0.25. In the compressed pellets, however, the intensity of the D band is enhanced, the I_D/I_G ratio increases to ~0.45. In addition, G band in raw SWCNT clearly shows a shoulder at low frequency due to splitting of tangential modes (known as G- and G+ bands) along the axis and on the perimeter of SWCNT [18]. This splitting of G band is not observed in the spectrum of the compressed SWCNT pellet of Fig. 3. The described changes of the Raman spectrum of SWCNT in the compressed pellet with respect to the ones observed in powder form reflects the state of stress and deformation that the SWCNT are subjected which is expected to depend on the pellet preparation pressure.

C. Thermoluminescent properties

The TL-signal is not enhanced as increasing pellet preparation pressure as shown in Fig. 4. The largest TL intensity of 13×10^4[nC] occurs for sample A, while for pellet B and C, the values were 34×10^4[nC] and 1×10^4[nC] respectively. Maximum TL response for all samples was found at 50 kGy. This indicates that with increasing pellet preparation pressure an increasing number of defects are created generating a decrease in the TL response. Therefore, C-C bonds in nanotubes are destroyed by energetic gamma photons generating defects. Once a critical defect concentration is reached, annihilation of defects may be energetically favourable. This process compensates for further defect generation and leads to the constant defect concentration even though irradiation doses increase. It is likely that the irradiation causes the formation of bonds between nanotubes, fixing their mutual positions [21].

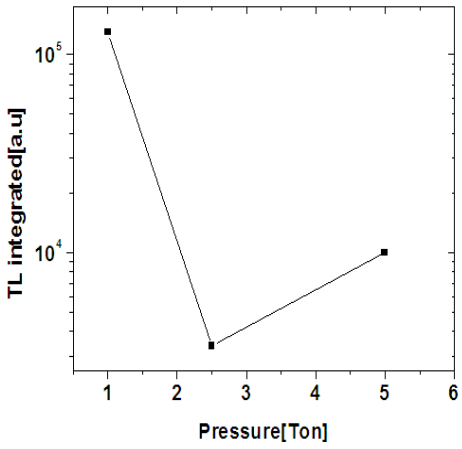

Fig. 4. TL-signal of pellets as function of preparation pressure.

1) Calculating kinetic parameters using computerized glow curve deconvolution (CGCD), peak shape and heuristic equations

The glow curves of samples A, B and C are composed of a broad peak between 350-500 K at different gamma doses and peaked at approximately in the 440–480 K range (Fig. 5.a, 5.b), evidently, it is not a single peak but rather a convolution of 3-4 peaks.

The maximum peak temperature (T_m) of the glow curves varying as function of dose and preparation pressure. At 50 kGy, is observed for preparation A, for a dose of 100 kGy, is exhibited for preparation B. A contrary effect is exhibited for sample C, as irradiation dose increase TL signal decrease, this behavior indicates the manufacturing pressure, impact in the number of defects and therefore in the intensity of TL response. This behavior could suggest that a continuous trap distribution occurred instead of a single trapping level responsible for the TL radiative emission [22]. The combination of irradiation-dose and preparation pressure modify trapping states. Therefore, are necessary carryout different methods for obtained kinetic parameters. In this case, CGCD, geometrical methods and heuristic equations will be used.

The glow curves in figure 5.a, 5.b were analyzed considering the general-order kinetics (GOK) model, which is most adequate because the samples exhibit a complex luminescence glow emission. However, there are other possibilities [23] to analyze the trapped charge distribution assuming a Gaussian or exponential distribution due to the thermal release of charge carriers from the trapping centers. Trap depths responsible for these peaks are correlated with energy states characterized by kinetic parameters such as: activation energy (E [eV]), frequency factor (s [s^{-1}]) and kinetic order (b). A decomposition of glow curves in individual glow peaks gives information about these parameters. The next equation has been modified according to the following glow peak algorithm:

$$I(T) = I_M (b)^{\frac{b}{b-1}} \exp\left(\frac{E}{kT}\frac{T-T_M}{T_M}\right)\left[(b-1)(1-\Delta)\frac{T^2}{T_M^2}\exp\left(\frac{E}{kT}\frac{T-T_M}{T_M}\right)+Z_M\right]^{\frac{-b}{b-1}} \quad (1)$$

Where I_M and T_M are the TL peak maximum intensity and peak maximum temperature, respectively, E *(eV)* the activation energy, b the kinetic order, and $\Delta_M = \frac{2kT_M}{E}$, $\Delta = \frac{2kT}{E}$ and $Z_M = 1+(b-1)\Delta_M$, with the pre-exponential factor given by $s = \frac{\beta E}{kT_M^2}\frac{1}{Z_M}\exp\left(\frac{E}{kT_M}\right)$. The curve fitting procedure was performed using the goodness of fit tested with a figure of merit (FOM) with a value equal or less than 5 % means a very good fit [24].

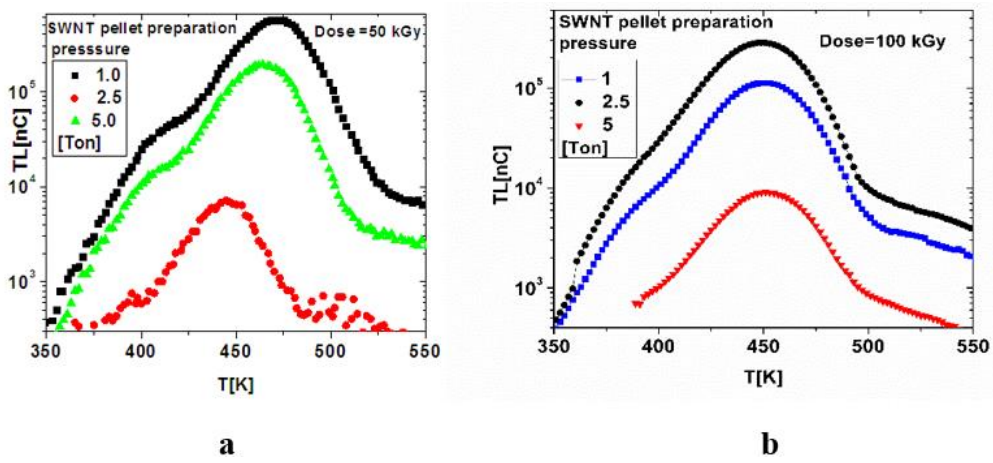

Fig. 5. Glow curves of SWCNT-pellets.

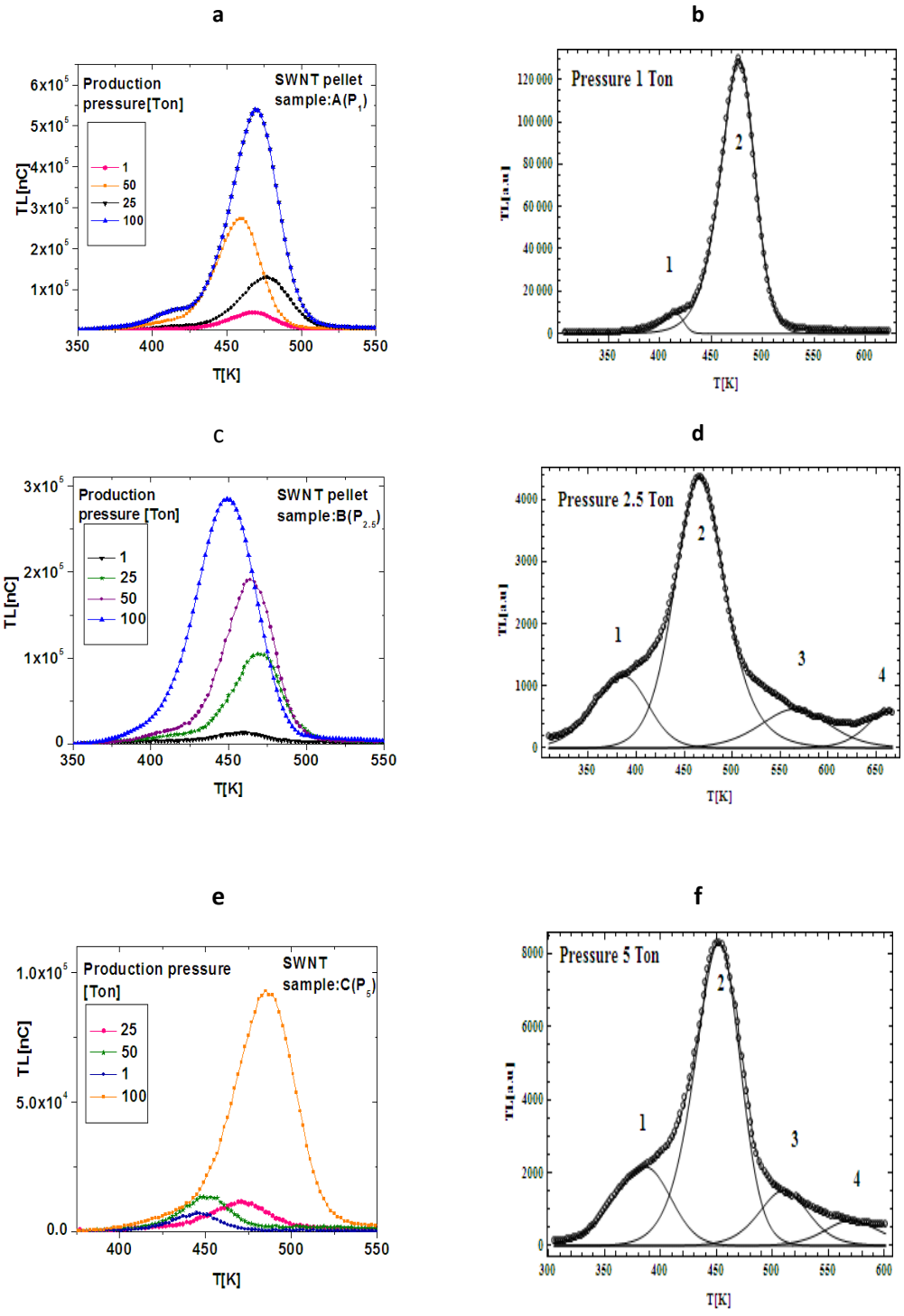

Fig. 6. Glow curves of SWNT-pellets, prepared at 1, 2.5 and 5 Ton. The doses were 1, 25, 50 and 100 kGy, 6.b, 6.d, 6.f) Computerized glow curve deconvolution (CGCD) using a general order model, the experimental glow curves (open circles) at delivered dose of 1 kGy..

From figures: 6.b, 6.d and 6.f, for all samples, the deconvoluted peaks #2, are in the temperature range 452-477 K and showed stability as a function of the dose, therefore peak #2 is chosen as main peak. In TL-dosimetry for personal, environmental, or clinical applications, a dosimetric peak generally lies in the 420–523 K temperature region [26] Trap activation energy have values in the 0.5–2.0 eV range for all samples. The deconvoluted first glow peak #1 has an activation energy 1.71 eV (pellet A), 0.5 eV (pellet B), and 0.5eV (pellet C) and correspond to the lower temperatures side (383–414 K) of the glow curves. The fourth peak #4 is assumed just to improve the FOM, but it has no physical meaning in pellets B and C. The kinetic parameters (activation energy ***E[eV]*** and frequency factor ***s [s^{-1}]***) of the pellets are listed in Table 2. For sample B, deconvoluted peak #2 is located at 452 K and has a kinetic order parameter (b) close to 2, indicating that trapping and re-trapping are the responsible process. As the manufacturing pressure of the SWNT pellets increases, the activation energy of the main peak decreases for all samples.

Summary of values of TL-signal and pellet preparation pressure. There is no linear correlation between preparation pressure and TL-signal. Preparation pressure effects on pellets is strongly marked on glow curve structures Fig. 5(a)-Fig. 5(b), with increasing preparation pressure, more energy states of traps are generated.

TABLE 1
PREPARATION PRESSURE DEPENDENCE OF TL-SIGNAL PARAMETERS.

Pellet	Preparation pressure [Ton]	Integrated TL signal [nC]	Deconvoluted glow peaks	Activation energy[eV] Peak 2
A	1	13×10^4	2	1.51
B	2.5	34×10^4	4	0.96
C	5	1.0×10^4	4	0.85

TABLE 2
KINETIC PARAMETERS AS OBTAINED BY THE COMPUTERIZED GLOW CURVE DECONVOLUTION (CGCD) USING GENERAL ORDER ALGORITHM.

Sample A (1 Ton)			FOM=0.05			
Peak	T[K]	E[eV]	b	s[s^{-1}]	α	R
1	414	1.71	1.20	1.62E+20		
2	477	1.51	1.51	1.71E+15	0.85	**0.25**
Sample B (2.5 Ton)			FOM=0.03			
Peak	T[K]	E[eV]	b	s[s^{-1}]		
1	385	0.50	1.30	264205		
2	452	0.96	1.90	2.95E+09	1	**0.75**
3	510	0.93	1.59	1.44E+07		
4	570	2.06	1.01	6.91E+14		
Sample C (5 Ton)			FOM=0.03			
Peak	T[K]	E[eV]	b	s[s^{-1}]		
1	383	0.5	1.22	291850		
2	465	0.85	1.36	1.84E+08	0.7	**0.15**
3	535	1.09	1.99	1.58E+09		
4	660	1.12	1.01	2.51E+10		

Peak #2 is a main peak.

The relationship among the α-values and b (kinetics order) showed that the overall scattering of the values found for b corresponding to any value found of α was within ±10% approximately[26]. The α-values for peak #2 of samples A, B and C were found to be in the 0.7–1.0 range. The activation energy values obtained with deconvolution for peak #2 are ranging between 0.85 to 1.5 [eV] (See Table 2), suggesting a possible good stability of the trapped charges produced during irradiation [26]. From new equations [27] a numerical relationship among b (kinetic order) and *R* has been established; where $R = \frac{A_n}{A_m} < 1$; and A_m recombination probability and A_n trapping probability.

The numerical value of *R* for samples A, B and C are in the 0.15 to 0.75 range concluding than trapping is a predominant process in glow curves of the analyzed samples. From kinetic parameters in Table 2, the values of b are different, for each sample, indicating the strong effect of manufacturing pressure in the kinetic order. Particularly, in the sample B, where b is almost two. Concluding, the preparation pressure of pellet C (5 Ton) changes the kinetic order. The activation energy values obtained from geometrical methods, are useful to comparing with deconvolution and dilucidated other mechanisms responsible of TL signal.

The value obtained of

$\mu_g = \frac{\delta}{\omega} = \frac{T_2 - T_M}{T_2 - T_1}$ ... (2) another important parameter is, $\tau = T_M - T_1$.

Chen equation is given by:

$$E_\alpha = c_\alpha \left(\frac{kT_M^2}{\alpha} \right) - b_\alpha (2kT_M) \quad (3)$$

Where α can be τ or ω and b_α, c_α has the next expressions:

$b_\tau = 1.58 + 4.2(\mu - 0.42)$, $\quad c_\tau = 1.51 + 3.0(\mu - 0.42)$,
$b_\delta = 0$ $\quad c_\delta = 0.976 + 7.3(\mu - 0.42)$,
$b_\omega = 1.0$, $\quad c_\omega = 2.52 + 10.2(\mu - 0.42)$,

where, *k* : Boltzmann constant=8.617 E-05 eV/K

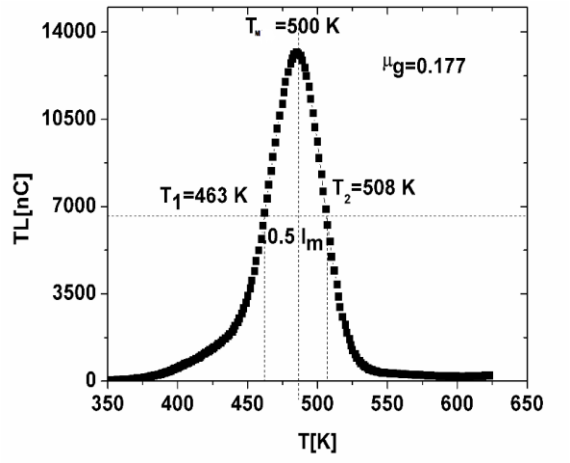

Fig. 7. SWCNT glow curve pellet and temperatures associated to geometrical method.

From Fig. 7 are obtained the geometrical values of α, τ, ω and μ_g to calculate activation energy using Chen, Grosswiener equations etc., and geometric factor respectively. These values are summarized in the next table.

From Table 3, is noticeable than value of activation energy(*E*) for peak 2, follows a first order kinetic for samples A and C, but in the case of sample B, is a second order, furthermore μ_g is independent of *E*, in the range from 0.1 to 1.6 eV.

TABLE 3
RESUME OF ACTIVATION ENERGY E AS OBTAINED AS BY PEAK SHAPE METHOD AND HEURISTIC EQUATIONS, FOR PEAK TWO.

Author	Equation	Sample A E[eV] μ_g=0.44	Sample B E[eV] μ_g=0.475	Sample C E[eV] μ_g=0.45
Grosswiener	E = 0.0462* τ	1.2936	0.9702	1.0164
Lushchik	E = 0.0649* δ	1.4278	1.2231	1.1684
Balarin	E = 0.0271* ω	1.355	1.084	1.084
Chen	3			
		1.2838	1.3167	1.0786
		1.3101	1.3276	1.1025
		1.3054	1.3311	1.0976

2) TL-dose response and linearity and non-linearity analysis

Three stages are displayed in the TL dose-response shown in Fig. 8. Linearity is observed up to 25 kGy (stage 1), and TL response increases between 20 to 50 kGy in stage 2. It seems that in stage 2, new traps are generated as consequence of the amount of irradiation. The TL response as function of dose for sample C exhibits a complex behavior from 50-100 kGy. The first action to understand the behavior of TL-dose response curve of a material is to find if TL of the material grows linearly as a function of dose. To carry out this action, we make use of an index called supralinearity *f(D)* which is given by the relation:

$$f(D) = \frac{\mathrm{M(D)/D}}{\mathrm{M(D_L)/D_L}} \tag{4}$$

$$\text{where, } M(D) = M_1\left[1 - \exp\left(-\frac{D}{E01}\right)\right] + M_2\left[1 - \left(1 + \frac{D}{E02}\right)\exp\left(-\frac{D}{E02}\right)\right] \tag{5}$$

Here M_1, M_2 are the TL signal contribution of each saturating exponential and $E01$, $E02$, are the saturation doses of each contribution. The $f(D)$ function may have the values; $f(D) > 1$ meaning supralinearity, $f(D) < 1$ meaning sublinearity and $f(D)$= 1, meaning linearity behavior. Another index $g(D)$ called superlinearity is commonly used to analyze linear and no linear behavior in the TL-dose response curves, and is given by:

$$g(D) = \frac{D\,M''(D)}{M'(D)} + 1 \tag{6}$$

The values of function $g(D)$ has different meanings: $g(D) > 1$ indicating superlinearity, $g(D) < 1$ sublinearity and $g(D)$= 1, linearity.

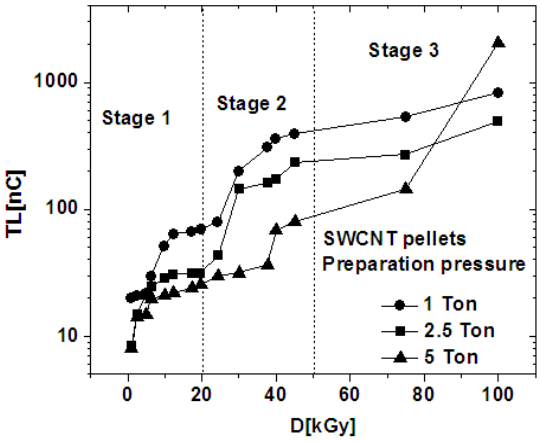

Fig. 8. Integrated thermoluminescence signal of SWCNT pellets as a function of dose.

As shown in Fig. 9, the behavior of *f(D)* is the same for samples B and C. Pellet A exhibits a supralinear tendency in all ranges analyzed, while for pellet C, sublinearity is predominant in the range 1 up to 5 kGy. A supra-sublinear tendency is presented by pellet B. In Fig. 9, superlinearity index *g(D)* also shows a similar behavior for pellets B and C, with an intense sublinearity occurring at the lowest dose. Meanwhile, pellet A shows sublinear-superlinear tendency.

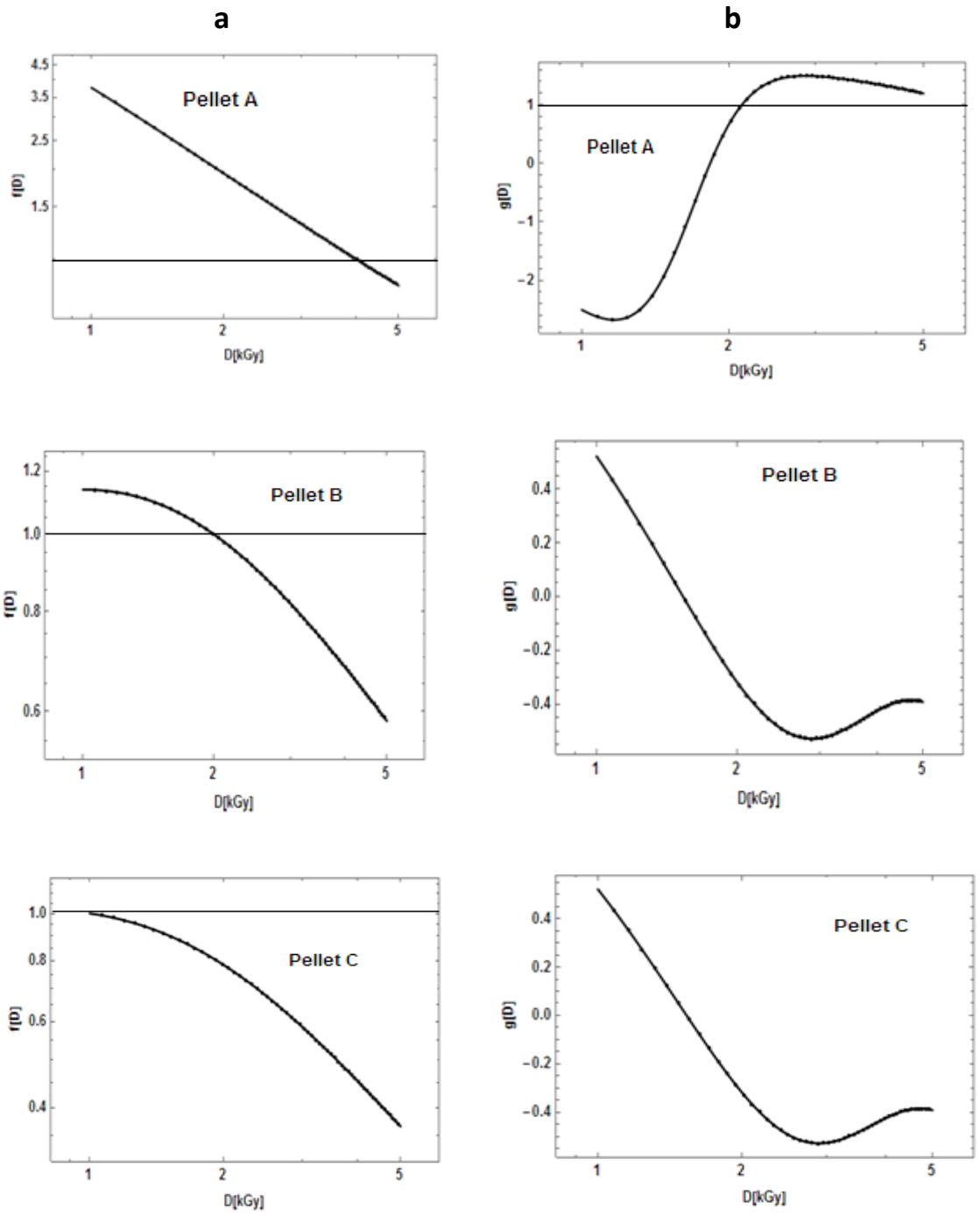

Fig. 9. Column a: Supralinearity f (D) index, Column b: Superlinearity g(D) index as a function of dose, for pellets A, B and C respectively.

IV. CONCLUSIONS

The experimental Raman spectra of samples indicate that SWCNT in the pellets end up in a state of stress and deformation as consequence of the application of pressure in pellet preparation. X-ray diffraction pattern of pellets after irradiation show an amorphous-like background as consequence of the creation of defects and partial amorphization of the SWCNT material. Pellets A, B and C analyzed in this work could be useful to measure high radiation fields given that they were tested at doses from 1.0 to 100 kGy. There is no difference in the number of trapping states generated between 2.5 and 5 Ton, in the glow curves, but there is a significantly difference in the TL-signals. A stable deconvoluted glow peak #2 appeared at 452, 465 and 477 K, for samples A, B and C, respectively. As pellet preparation pressure increases, activation energy decreases for all traps in the samples, indicating perhaps a decrease in the number of defects. The manufacturing pressure of pellets induce changes in the kinetic order. Finally pellet A is a promising TL-detector with usability at high gamma fields.

CRediT (*Contributor Roles Taxonomy*)

Author Contributions: **Author Contributions**: Conceptualization: A**OM**, J**OL**, B**LA,** R**GA**; Methodology: A**OM**, J**OL**, B**LA,** R**GA**; Software: A**OM**; Investigation: A**OM**, J**OL**, B**LA,** R**GA**; Writing-original draft preparation: A**OM**; Writing-review and editing: A**OM**; Supervision: A**OM**, J**OL**, B**LA,** R**GA**; Formal analysis: A**OM**, J**OL**, B**LA,** R**GA**; Project administration: A**OM** ; Funding acquisition: A**OM**, J**OL**, B**LA,** R**GA**.

Acknowledgments: A. Ortiz-Morales acknowledge EDD-IPN 2025 for support and L.V.O-R and D.I.O-R, J. O-L acknowledges COFAA-IPN and EDI-IPN for academic scholarships and SIP-IPN for partial financial support through project number SIP-20210038. R.G-A acknowledge SIP-IPN for support through project number 20210036 and COFAA-IPN academic scholarship.

Conflicts of Interest: The authors declare no conflicts of interest.

Data Availability Statement: Data available upon request.

Funding: No external funding was received for this work.

REFERENCES

[1] A. Ortiz-Morales, M. García Hipólito, E. Cruz Zaragoza, R. Gómez Aguilar, "Characterization and thermoluminescence study of gamma irradiated Tb-doped ZnO and undoped ZnO synthesized by spray pyrolysis method", *Nova scientia*, vol. 13, no. 27, pp. 1-25, 2021. https://doi.org/10.21640/ns.v13i27.2877

[2] A. Ortiz-Morales, J. Ortiz-Lopez, E. Cruz-Zaragoza, R. Gómez-Aguilar, "Thermoluminescence and photoluminescence analyses of MEH-PPV, MDMO-PPV and RU(bpy) 3 gamma-irradiated polymer thin films", *Applied Radiation and Isotopes*, no. 102, pp. 55–62, 2015. https://doi.org/10.1016/j.apradiso.2015.04.013

[3] A. Ortiz-Morales, R. Gómez-Aguilar, J. Ortiz-Lopez, E. Cruz-Zaragoza, "Characterizing the Dosimetric Properties of MEH-PPV Using Thermoluminescence (TL)", *MRS Proceedings*, vol. 1613, pp. 127-131, 2014. https://doi.org/10.1557/opl.2014.169

[4] A. Ortiz-Morales, J. Ortiz-López, B. Leal-Acevedo, R. Gómez-Aguilar, "Thermoluminescence of single wall carbon nanotubes synthesized by hydrogen-arc-discharge method", *Applied Radiation and Isotopes*, vol. 145, pp. 32-38, 2019. https://doi.org/10.1016/j.apradiso.2018.11.001

[5] L. Aparecida Forner, C. Viccari, P. Nicolucci, "Dosimetric properties of thermoluminescent pellets of $CaSO_4$ doped with rare earths at low doses", *Radiation Physics and Chemistry*, vol. 171, 2020. https://doi.org/10.1016/j.radphyschem.2020.108704

[6] V. K. Mathur, A. C. Lewandowski, N. A. Guardala, J. L. Price. "High dose measurements using thermoluminescence of $CaSO_4$:Dy", *Radiation Measurements* vol. 30 no. 6, pp. 735-738, 1999. https://doi.org/10.1016/S1350-4487(99)00244-9

[7] M. A. Tarawneha, S. A. Saraireha, R. Shan Chenb, S. Hj Ahmad, M. A. Al-Tarawni, L. Jiun Yu, "Gamma irradiation influence on mechanical, thermal and conductivity properties of hybrid carbon nanotubes/montmorillonite nanocomposites", *Radiation Physics and Chemistry*, vol. 179, 2021. https://doi.org/10.1016/j.radphyschem.2020.109168

[8] J. Sobczak, A. Truszkiewicz, K. Cwynar, S. Ruczka, A. Kolanowska,R. G. Jedrysiak, S. Waskiewicz, M. Dzida, S. Boncel, G. Zyła "Soft, ternary, X- and gamma-ray shielding materials: paraffin-based iron-encapsulated carbon nanotube nanocomposites", *Mater. Adv.*, no. 18, 2024. https://doi.org/10.1039/d4ma00359d

[9] M. G. Albarrán Sánchez, E. Mendoza Villavicencio, E. Cruz Zaragoza, "Dosimetría Química de irradiadores gamma de ^{60}Co y ^{137}Cs de uso semi-industrial e investigación", *Nova Scientia*, vol. 9 no. 19, pp. 113, 2017. https://doi.org/10.21640/ns.v9i19.943

[10] J. Sippel-Oakley, H. T. Wang, B.S. Kang, Z. Wu, F. Ren, A.G. Rinzler, S.J. Pearton, "Carbon nanotube films for room temperature hydrogen sensing", *Nanotechnology*, vol. 16 no. 10, pp. 2218–2221, 2005. https://doi.org/10.1088/0957-4484/16/10/040

[11] X. W. Tang, Y. Yang, W. Kim, Q. Wang, P. Qi, H. Dai, L. Xing, "Measurement of ionizing radiation using carbon nanotube field effect transistor", *Physics in Medicine and Biology*, vol. 50 no. 3, pp. N23–N31. https://doi.org/10.1088/0031-9155/50/3/N02

[12] V.N. Khabashesku, W. E. Billups, J. L. Margrave, "Fluorination of Single-Wall Carbon Nanotubes and Subsequent Derivatization Reactions", *Accounts of Chemical Research*, vol. 35 no. 12, pp. 1087–1095, 2002. https://doi.org/10.1021/ar020146y

[13] S. M. Bachilo, M.S. Strano, C. Kittrell, R. H. Hauge, R.E. Smalley, R.B. Weisman, "Structure-Assigned Optical Spectra of Single-Walled Carbon Nanotubes", *Science*, vol. 298, pp. 2361–2366, 2002. https://doi.org/10.1126/science.1078727

[14] M. X. Pulikkathara, M. L. Shofner, R. T. Wilkins, J. G Vera, E. V. Barrera, F. J. Rodríguez-Macías, R.K Vaidyanathan, C. E. Green, C. G. Condon, "Fluorinated Single Wall Nanotube/Polyethylene Composites for Multifunctional Radiation Protection", *MRS Proceedings*, vol. 740, 2002. https://doi.org/10.1557/PROC-740-I11.6

[15] B. Khare, M. Meyyappan, M. Moore, P. Wilhite, H. Imanaka, B. Chen, "Proton Irradiation of Carbon Nanotubes", *Nano Letters*, vol. 3 no. 5, pp. 643–646, 2003. https://doi.org/10.1021/nl034058y

[16] T. S. Gspann, N. H. H. Ngern, A. Fowler, A. H. Windle, V.B.C. Tan, J. A. Elliott, "Triboluminescence flashes from high-speed ruptures in carbon nanotube Macro-Yarns", *Materials Letters*, vol. 213, pp. 298–302, 2018. https://doi.org/10.1016/j.matlet.2017.11.066

[17] S. M. Bachilo, M. S. Strano, C. Kittrell, R. H. Hauge, R. E. Smalley, R.B. Weisman "Structure-Assigned Optical Spectra of Single-Walled Carbon Nanotubes", *Science*, vol. 298 no. 5602, pp. 2361–2366, 2002. https://doi.org/10.1126/science.1078727

[18] V. Cruz-Alvarez, J. Ortiz-López, C. Mejía-García, J.S. Arellano-Peraza, V.M. Sánchez-Martínez, J. Chávez-Carvayar, "Anisotropies in Carbon Nanotube Synthesis by the Hydrogen Arc Plasma Jet Method", *Fullerenes, Nanotubes and Carbon Nanostructures*, vol. 13 no. 4, pp. 299–311, 2005. https://doi.org/10.1080/15363830500237143

[19] T. M. Keller, S. B. Qadri, C. A. Little, "Carbon nanotube formation in situ during carbonization in shaped bulk solid cobalt nanoparticle compositions", *J. Mater. Chem.*, vol. 14, pp. 3063-3070, 2004.

[20] T. Shimada, T. Sugai, C. Fantini, M. Souza, L. G. Cançado, A. Jorio, M.A. Pimenta, R. Saito, A. Grüneis, G. Dresselhaus, M.S. Dresselhaus, Y. Ohno, T. Mizutani, H. Shinohara, "Origin of the 2450cm−1 Raman bands in HOPG, single-wall and double-wall carbon nanotubes", *Carbon*, vol. 43 no. 5, pp. 1049–1054, 2005. https://doi.org/10.1016/j.carbon.2004.11.044

[21] V. Skákalová, "Effect of Gamma-Irradiation on Single-Wall Carbon Nanotube Paper", *AIP Conference Proceedings*, vol. 685, pp. 143–147, 2003. https://doi.org/10.1063/1.1628005

[22] E. Cruz-Zaragoza, B. Ruiz-Gurrola, C. Wacher, T. Flores-Espinoza, M. Barboza-Flores, "Gamma radiation effects in coriander (Coriandrum sativum L) for consumption in Mexico", *Rev. Mex. Fís.*, vol. 57, pp. 80-86, 2011.

[23] G. Kitis, J. M. Gomez-Ros, J. W. N. Tuyn, "Thermoluminescence glow-curve deconvolution functions for first, second and general orders of kinetics", *Journal of Physics D: Applied Physics*, vol. 31, 1998. http://doi/10.1088/0022-3727/31/19/037

[24] H. G. Balian, N. W. Eddy, "Figure-of-merit (FOM), an improved criterion over the normalized chi-squared test for assessing goodness-of-fit of gamma-ray spectral peaks" *Nuclear Instruments and Methods*, vol. 145 no. 2, pp. 389–395, 1977. https://doi.org/10.1016/0029-554X(77)90437-2

[25] C. Sunta, W.E. Ayta, J.F. Chubaci, S. Watanabe, "General order and mixed order fits of thermoluminescence glow curves—a comparison", *Radiation Measurements*, vol. 35 no. 1, pp. 47–57, 2002. https://doi.org/10.1016/S1350-4487(01)00257-8

[26] G. Kitis, V. Pagonis, S. E. Tzamarias, "The influence of competition effects on the initial rise method during thermal stimulation of luminescence: A simulation study", *Radiation Measurements*, vol. 100, pp. 27–36, 2017. https://doi.org/10.1016/j.radmeas.2017.03.047

[27] H. A. Borbón-Nuñez, C. Furetta, "Activation Energy of Modified Peak Shape Equations", *World Journal of Nuclear Science and Technology*, vol. 7 no. 4, pp. 274–283, 2017. https://doi.org/10.4236/wjnst.2017.74021